

COMPARATIVE EVALUATION OF DIFFERENT DAMAGE MEASURES FOR REINFORCED CONCRETE BUILDINGS CONSIDERING VARIABLE INCIDENT ANGLES

Konstantinos Morfidis¹, Konstantinos Kostinakis², and Christos Karakostas³

¹Earthquake Planning and Protection Organization (EPPO-ITSAK)
5 Ag. Georgiou Str., 55535, Thessaloniki, Greece
e-mail: kmorfidis@itsak.gr

²Department of Civil Engineering, Aristotle University of Thessaloniki
Aristotle University campus, 54124, Thessaloniki, Greece
e-mail: kkostina@civil.auth.gr

³Earthquake Planning and Protection Organization (EPPO-ITSAK)
5 Ag. Georgiou Str., 55535, Thessaloniki, Greece
e-mail: christos@itsak.gr

Keywords: Reinforced Concrete Structures, Damage Index, Seismic analysis, Seismic excitation angles, Seismic Damage, Inelastic response.

Abstract. *One way of quantifying the extent of seismic damage induced to Reinforced Concrete (R/C) structures is the use of damage indices. Various damage indices have been introduced by many researchers incorporating different parameters for estimating structural damage. The aim of the present paper is the comparative evaluation of three of the most widely used damage indices for the R/C buildings taking into account the orientation of the strong motion. For the investigation of the present study three symmetric in plan R/C buildings are investigated: a low-rise building (3 stories), a medium-rise building (5 stories) and a high-rise building (8 stories). The three buildings are analysed by nonlinear time-history analysis using 20 bi-directional earthquake ground motions. The two horizontal accelerograms of each ground motion are applied along horizontal orthogonal axes forming 72 different angles with the structural axes. For each ground motion and incident angle, the local damage indices at every relevant cross section as well as the overall damage index of the building are computed using three different definitions of the damage index. The analyses results show that the numerical estimation of the seismic damage induced to R/C buildings depends on the damage index used to quantify the damage. Moreover, the overall damage state of the building is significantly affected by the incident angle of the ground motion.*

1 INTRODUCTION

The assessment of the level of the damages that is expected to come up in structural members of R/C buildings constitutes a very important piece of data in the process of planning scenarios of seismic risk of individual buildings as well as of a group of buildings. The procedures available nowadays are based on analytical methods, as well as in situ assessments of seismic vulnerability, or on a combination of both. One of the analytical methods available is based on use of suitable damage indices. Damage indices are analytical expressions of the damage level expected to appear in structural members and are generally defined in various ways in international literature. Their basic principle is the assessment of the damage level through its correlation with parameters that can be calculated analytically. Such parameters are ductility, strength, the reinforcement ratio, the hysteresis loop etc. Due to the fact that the inelastic response of structural elements that causes damages depends on a number of factors which cannot be easily taken into consideration simultaneously, several definitions of damage indices have been proposed. Among the various factors that affect the reliable analytical evaluation of damage indices, one should highlight the uncertainty introduced in the response of buildings by the seismic excitation angle. Research has shown (see e.g. [1, 2, 3, 4]) that in many cases the seismic excitation angle can radically alter the analysis results in terms of both the required reinforcement ratio of structural members (see e.g. [1, 4]) and of the damage level (see e.g. [2, 3]).

The objective of the present paper is the investigation of the level of the expected damages in R/C buildings by applying three different definitions of the damage index, i.e. the definitions of Park-Ang [5, 6], Bracci et al. [7] and Cosenza et al. [8]. The evaluation of these indices requires non-linear time-history analyses. The accelerograms demanded for these analyses were selected out of 20 different recordings, 10 of which correspond to near-fault strong motion records, while the rest correspond to far-fault records. This specific distinction was chosen since it is well-known that far-fault records have characteristics different from those of near-fault ones, resulting in a difference in the seismic response of buildings. With regard to the choice of the buildings, three R/C double symmetric buildings of low (3-storey), medium (5-storey) and high (8-storey) rise were selected. The rationale behind this choice was the investigation of the influence of the horizontal stiffness on the damage level in connection with the different characteristics of earthquakes. All selected buildings have a structural system which is a frame system along one direction and a wall-equivalent dual system along the other direction (which is perpendicular to the former), with walls that receive approximately 60% of the base shear of buildings in this specific direction. This choice was made in order to investigate the influence of the seismic excitation angle on buildings with horizontal stiffnesses that are considerably different along two perpendicular directions. The buildings were designed following the provisions of EN1992-1-1 [9], and EN1998-1 [10]. Then the buildings were analyzed by nonlinear time-history analysis for each one of the 20 earthquake records taking into account 72 different incident angles of the input motion. For each ground motion and incident angle the overall damage index of the three buildings was computed using the three aforementioned different definitions of damage indices.

The analyses results show that the use of Bracci et al. damage index leads to the largest values of the overall structural damage index of the buildings, whereas the use of Cosenza et al. damage index leads to the smallest values for the vast majority of the incident angles and earthquake records. Moreover, the most widely used Park and Ang damage index leads to the smallest influence of the excitation angle as well as of the number of stories.

2 DESCRIPTION OF THE PROCEDURE OF THE ANALYSIS

The procedure followed in order to achieve the goals of the present investigation consists of the following steps:

- (a) Selection of the examined R/C buildings,
- (b) Modeling of the elastic and inertia behavior,
- (c) Design of the structural elements of the buildings,
- (d) Modeling of the nonlinear behavior of the structural elements of the buildings,
- (e) Selection of the seismic excitations used for the nonlinear analyses,
- (f) Analysis of the buildings using the method of nonlinear time-history analysis for various angles of the seismic excitation,
- (g) Calculation of damage indices for the structural elements, as well as for each building as a whole, with three different definitions of damage indices.

In the following, the details of the aforementioned steps are presented.

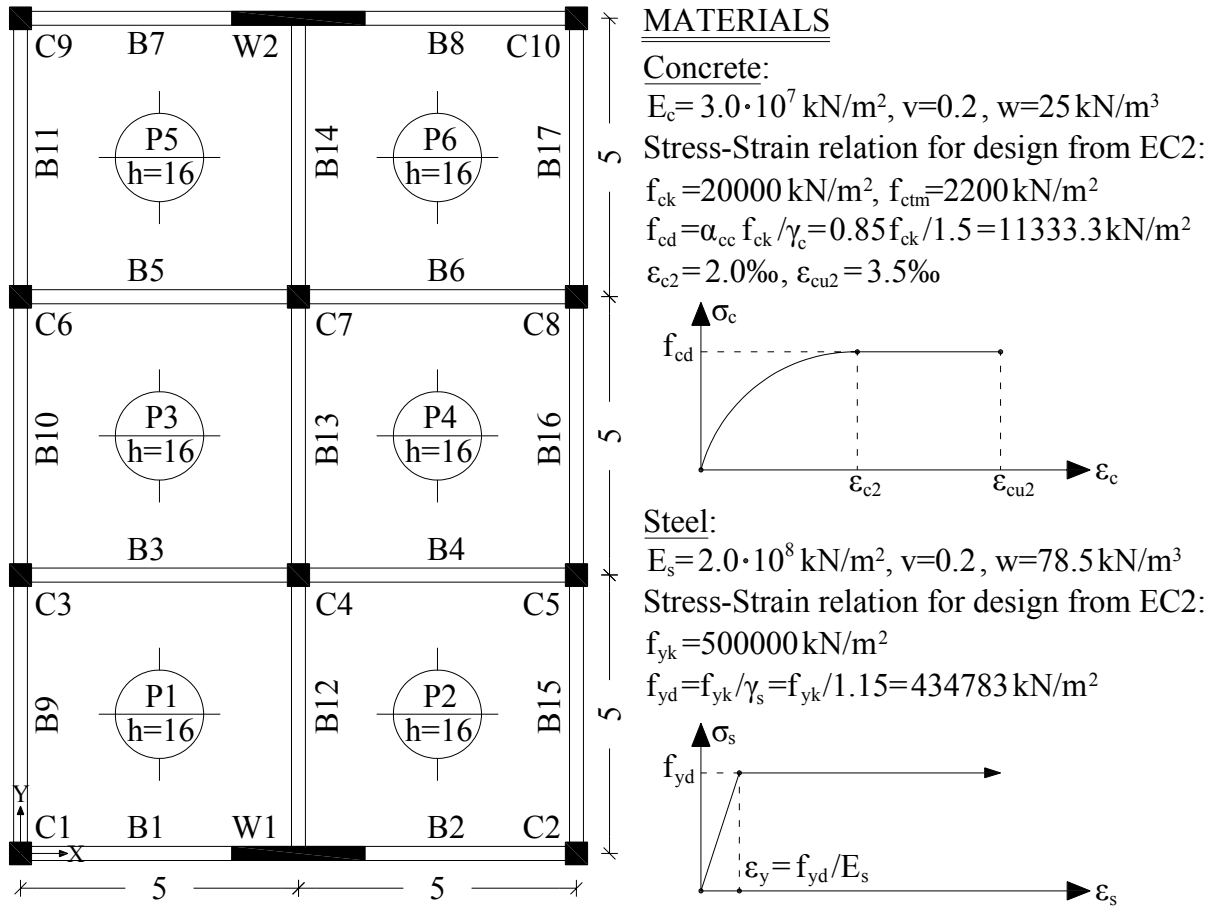
2.1 Description of the selected R/C buildings and assumptions of their elastic modeling

For the purposes of the investigation, three double symmetric R/C buildings, with design parameters as shown in Figure 1, were chosen. All three buildings have a structural system that consists of R/C frames in two orthogonal directions (axes X and Y). Along X-axis there are two R/C walls that receive approximately 60% of the base shear. According to the structural types described in EN1998-1 ([10], §5.2.2.1), all buildings belong to the type of frame systems along the Y-axis and to the type of wall-equivalent dual systems along X-axis. Therefore, their horizontal stiffness along the Y-axis is roughly equal to 65% of their horizontal stiffness along the X-axis. All buildings are regular in plan and elevation according to the criteria set by EN1998-1 ([10], §4.2.3.2, §4.2.3.3), and were designed as medium ductility class (DMC) buildings. Based on the above data, the process of calculating the upper limit value of the behavior factor q of EN1998-1 ([10], §5.2.2.2) led, in all three cases, to the values $\max q_x=3$ and $\max q_y=3.9$. However, a unique value for the X and Y axes, equal to $q=\min(\max q_x, \max q_y)=3$, was taken in to account for the analysis and design.

In the modeling of the buildings, all basic recommendations of EN1998-1 [10] were taken into consideration, such as the diaphragmatic behavior of the plates, the rigid zones in the joint regions of beams/columns and beams/walls, and the values of flexural and shear stiffness corresponding to cracked R/C elements. All buildings were considered to be fully fixed to the ground.

2.2 Analysis and design of the buildings

The buildings were analyzed using the modal response spectrum analysis, as defined in EN1998-1 ([10], §4.3.3.3). The R/C structural elements were designed following the provisions of EN1992-1-1 [9] and EN1998-1 [10]. Consequently, a capacity design at frame joints was made only along Y-axis, where the buildings belong to the type of frame systems ([10], §4.4.2.3[5]). It should be noted that the choice of the dimensions of the structural element cross-sections as well as that of their reinforcement was made while bearing in mind the optimum exploitation of the structural materials (steel and concrete). Therefore, the capacity ratios (CRs) of all critical cross-sections due to bending and shear are close to 1.0 (the mean value of CRs ranges between 0.92-0.96). The professional program for R/C building analysis and design RAF [11] was employed in both the analysis and the design.



Design spectrum for elastic analysis: From paragraph 2.2.2.5 of EC8-1. Parameters:

Reference peak ground acceleration $a_{gR} = 0.24g$ $\rightarrow a_g = \gamma_I a_{gR} = 0.24g$

Importance class of buildings: II $\rightarrow \gamma_I = 1.0$

Ground type: C $\rightarrow S = 1.15$, $T_B = 0.2 \text{ sec}$, $T_C = 0.6 \text{ sec}$, $T_D = 2.5 \text{ sec}$

Value of the behaviour factor $q = 3$

Dimensions of the cross-sections of R/C members:

Storey	3-Story Building (3SB)			5-Story Building (5SB)			8-Story Building (8SB)		
	Beams	Columns	Walls	Beams	Columns	Walls	Beams	Columns	Walls
1 st	25/45	35/35	115/25	25/55	40/40	150/25	25/55	45/45	160/25
2 nd	25/45	35/35	115/25	25/55	40/40	150/25	25/55	45/45	160/25
3 rd	20/45	30/30	115/25	25/50	35/35	150/25	25/55	40/40	160/25
4 th	—	—	—	25/45	35/35	150/25	25/50	40/40	160/25
5 th	—	—	—	20/45	30/30	150/25	25/50	35/35	160/25
6 th	—	—	—	—	—	—	25/50	35/35	160/25
7 th	—	—	—	—	—	—	25/45	30/30	160/25
8 th	—	—	—	—	—	—	20/45	30/30	160/25

Figure 1: Design parameters of the investigated buildings

2.3 Selection of the seismic excitations used for the nonlinear time-history analyses

A suite of 20 pairs of horizontal bi-directional earthquake ground motions (10 far-fault and 10 near-fault records) obtained from the PEER [12] and the European [13] strong motion database was used as input ground motion for the analyses of the buildings investigated in the present study. The ground motions were recorded on Soil Type C according to EN1998-1. The characteristics of the input ground motions are shown in Tables 1 and 2 along with the correlation factor of the components. The correlation factor ρ is given [14] by Eq. 1:

$$\rho = \frac{\sigma_{xy}}{(\sigma_{xx} \cdot \sigma_{yy})^{1/2}} \quad \text{with} \quad \sigma_{ij} = \frac{1}{s} \cdot \left(\int_0^s \alpha_i(t) \cdot \alpha_j(t) dt \right) \quad i = x, y \quad (1)$$

where $\alpha_x(t)$ and $\alpha_y(t)$ are the recorded ground accelerations along the two horizontal directions of the ground motion; σ_{xx} , σ_{yy} are quadratic intensities of $\alpha_x(t)$ and $\alpha_y(t)$ respectively; σ_{xy} is the corresponding cross-term; s is the duration of the motion.

It should be noted that, as ASCE 41-06 proposes [15], the uncorrelated horizontal components of ground motion have been used as seismic input in the present study. The accelerograms were scaled to Peak Ground Acceleration $PGA = a_g \cdot S = 0.276g$, where a_g and S are the design ground acceleration and the soil factor respectively used for the elastic analysis of the buildings. Although it is known that PGA scaling does not correlate strongly with the expected damage levels, it was nevertheless applied herein for simplicity reasons, since in the present study the factor under investigation is, as already mentioned, the incident angle of the input motion. In Tables 1 and 2 the scale factors (SF) produced by the scaling procedure for each ground motion are presented. The SRSS of the 5%-damped spectra of the scaled accelerograms are depicted in Figures 2a and 2b.

No	Date	Earthquake name	Magnitude	Station name	Station number	Closest distance (Km)	Component (deg)	PGA (g)	Cor Factor (p)	SF
1	24/4/1984	Morgan Hill	6.2 (Ms)	Capitola	47125	38.1	042 132	0.099 0.142	0.26	2.40
2	1/10/1987	Whittier Narrows	6 (Ms)	LA - Hollywood Stor FF	24303	25.2	000 090	0.221 0.124	-0.09	1.67
3	17/1/1994	Northridge	6.7 (Ms)	Compton - Castlegate St	90078	49.6	000 270	0.088 0.136	-0.01	2.51
4	17/1/1994	Northridge	6.7 (Ms)	Downey - Birchdale	90079	40.7	090 180	0.165 0.171	0.24	1.90
5	17/1/1994	Northridge	6.7 (Ms)	LA - Saturn St	90091	30	020 110	0.474 0.439	-0.06	0.61
6	6/8/1979	Coyote Lake	5.7 (Ms)	Halls Valley	57191	31.2	150 240	0.039 0.050	0.15	6.90
7	2/5/1983	Coalinga	6.4 (Ms)	Parkfield - Cholame 5W	36227	47.3	270 360	0.147 0.131	-0.10	2.00
8	8/7/1986	N. Palm Springs	6 (Ms)	Indio - Coachella Canal	12026	45.7	000 090	0.053 0.050	0.09	5.52
9	13/6/1993	Mouzakiiika (Greece)	5.3 (Mw)	Lefkada-OTE Building	8	33	LONG TRAN	0.043 0.146	-0.39	3.21
10	15/4/1979	Montenegro	6.9 (Mw)	Stolac-PPD	2967	107	N-S W-E	0.034 0.042	0.02	6.99

Table 1: Far-fault ground motion records

No	Date	Earthquake name	Magnitude	Station name	Station number	Closest distance (Km)	Component (deg)	PGA (g)	Cor Factor (p)	SF
1	1/10/1987	Whittier Narrows	6 (Ms)	El Monte - Fairview Av	90066	9.8	000 270	0.120 0.228	0.23	1.49
2	20/9/1999	Chi-Chi, Taiwan	7.6 (Ms)	CHY	028	7.31	N W	0.821 0.653	-0.07	0.37
3	18/10/1989	Loma Prieta	6.9 (Ms)	Gilroy Array #3	47381	14.4	000 090	0.555 0.367	0.05	0.61
4	17/1/1994	Northridge	6.7 (Ms)	Simi Valley - Katherine Rd	90055	14.6	000 090	0.877 0.640	-0.02	0.36
5	1/10/1987	Whittier Narrows	6 (Ms)	LA - E Vernon Ave	90025	10.8	083 173	0.146 0.175	-0.09	1.67
6	1/10/1987	Whittier Narrows	6 (Ms)	LA - Fletcher Dr	90034	14.4	144 234	0.171 0.231	-0.04	1.45
7	11/9/1976	Friuli (Italy)	5.5 (Mw)	Buia	33	7	E-W N-S	0.105 0.230	0.04	1.64
8	24/2/1981	Aktion (Greece)	6.6 (Mw)	Korinthos-OTE Building	121	10	N30 N120	0.230 0.310	-0.28	1.03
9	26/9/1997	Umbria Marche (Italy)	6 (Mw)	Colfiorito	221	5	N-S W-E	0.199 0.223	-0.11	1.43
10	7/9/1999	Ano Liosia (Greece)	6 (Mw)	Athens-Neo Psihiko	1253	8	LONG TRANS	0.083 0.101	-0.05	3.00

Table 2: Near-fault ground motion records

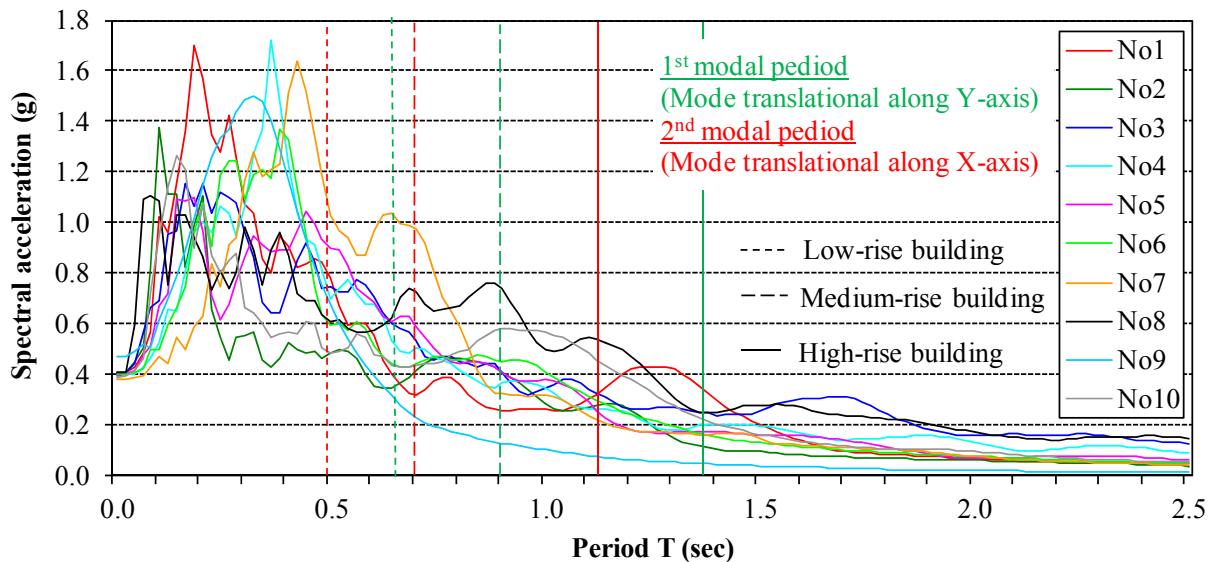


Figure 2a: SRSS of the 5%-damped spectra of the scaled accelerograms corresponding to far-fault records

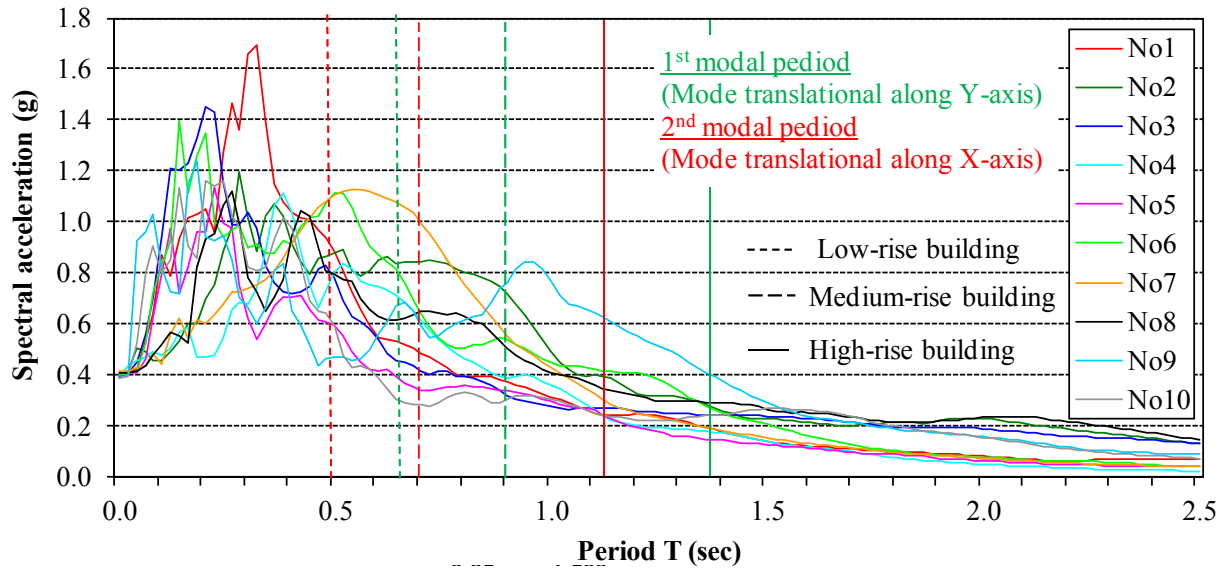


Figure 2b: SRSS of the 5%-damped spectra of the scaled accelerograms corresponding to near-fault records

2.4 Modeling of the nonlinear behavior and analysis of the buildings

Plastic hinges, which are located at the column and beam ends as well as at the base of the walls, were used to model the material inelasticity of the members by means of a Modified Takeda hysteresis model [16] (Figure 3(a)), where for the parameters α and β the values of 0.25 and 0 for the beams and 0.50 and 0 for the vertical frame elements were used [17]. It is important to notice that the effects of axial load-biaxial bending moments (P-M-M) interaction at column and wall hinges were taken into consideration by means of the P-M-M interaction diagram shown in Figure 3(b), which was implemented in the software used to conduct the analyses [18]. The plastic moments as well as the parameters needed to determine the P-M-M interaction diagram of the vertical elements' cross sections (Figure 3(b)) were calculated using appropriate software [19].

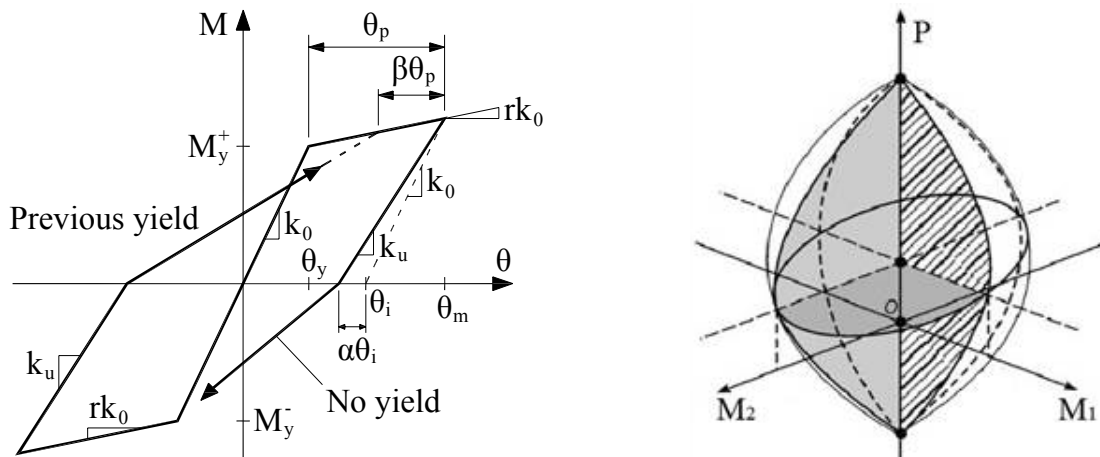


Figure 3: Moment (M) - Rotation (θ) relationship (a) and P-M-M interaction diagram [18] (b)

The three buildings were then analyzed by Nonlinear Time-History Analysis (NTHA) for each one of the 20 earthquake ground motions. The analyses were performed with the aid of the computer program RUAUMOKO [18]. Furthermore, as the seismic incident angle with regard to structural axes is unknown, the two horizontal accelerograms of each ground motion

were applied along horizontal orthogonal axes forming with the structural axes consecutive angles of $\theta=0^\circ, 5^\circ, 10^\circ, \dots, \dots, 355^\circ$. Thus for each building and each pair of accelerograms 72 different incident angles of the input motion were considered. As a consequence a total of 4,320 NTHA (3 buildings x 20 earthquake records x 72 incident angles) were conducted in the present study.

2.5 Calculation of damage indices

For each ground motion and incident angle, the local damage indices at every relevant cross section (columns' and beams' ends and at the bases of the walls) as well as the overall damage index of each one of the three buildings were computed. In particular, three different damage indices were considered: the Park and Ang damage index [5] modified by Kunnath et al. [6], the Bracci et al damage index [7] and the Cosenza, et al. damage index [8]. Note that the aforementioned local damage indices have been widely used for the inelastic assessment of structures [8, 20, 21, 22, 23].

More specifically, at a given cross section the local damage index (LDI) according to Park and Ang, Bracci et al. and Cosenza et al. is given by Eqs. 2, 3 and 4 respectively:

$$LDI^{\text{Park-Ang}} = \frac{\phi_m - \phi_y}{\phi_u - \phi_y} + \left(\frac{\beta}{M_y \cdot \phi_u} \right) \cdot E_T \quad (2)$$

$$LDI^{\text{Bracci et al.}} = \frac{E_m}{E_u} \quad (3)$$

$$LDI^{\text{Cosenza et al.}} = \frac{\mu_m - 1}{\mu_u - 1} \quad (4)$$

where ϕ_m is the maximum curvature observed during the load history, ϕ_u is the ultimate curvature capacity, ϕ_y is the yield curvature, μ_m is the maximum ductility demand, μ_u is the maximum allowable value of the ductility, E_T is the dissipated hysteretic energy, E_m is the work done at maximum curvature, E_u is the work done at ultimate curvature, M_y is the yield moment of the cross section and β is a dimensionless constant determining the contribution of cyclic loading to damage, which is taken equal to 0.5 for the analyses conducted in the present study.

Moreover, the overall structural damage index (OSDI) of the building was computed as a weighted average of the local damage indices at the ends of each element. The dissipated energy was used as a weight factor (Eq. 4) [20, 24, 25]:

$$OSDI = \sum_{i=1}^n \left[LDI_i \cdot \left(E_{Ti} / \sum_{i=1}^n E_{Ti} \right) \right] \quad (5)$$

where LDI_i is the local damage index at cross section i determined by Eqs. 2, 3 or 4, E_{Ti} is the energy dissipated at cross section i and n is the number of cross sections at which the local damage is computed.

3 RESULTS OF THE ANALYTICAL INVESTIGATIONS

Figure 4 presents the variation of the OSDI with the incident angle under the No9 far-fault and No10 near-fault earthquake records (see Tables 1 and 2) for the three buildings investigated in the present study. We can see that the near-fault record leads to larger values of damage indices for the majority of incident angles than the corresponding values produced by the far-fault ground motion. This observation is more evident for the 3-story building.

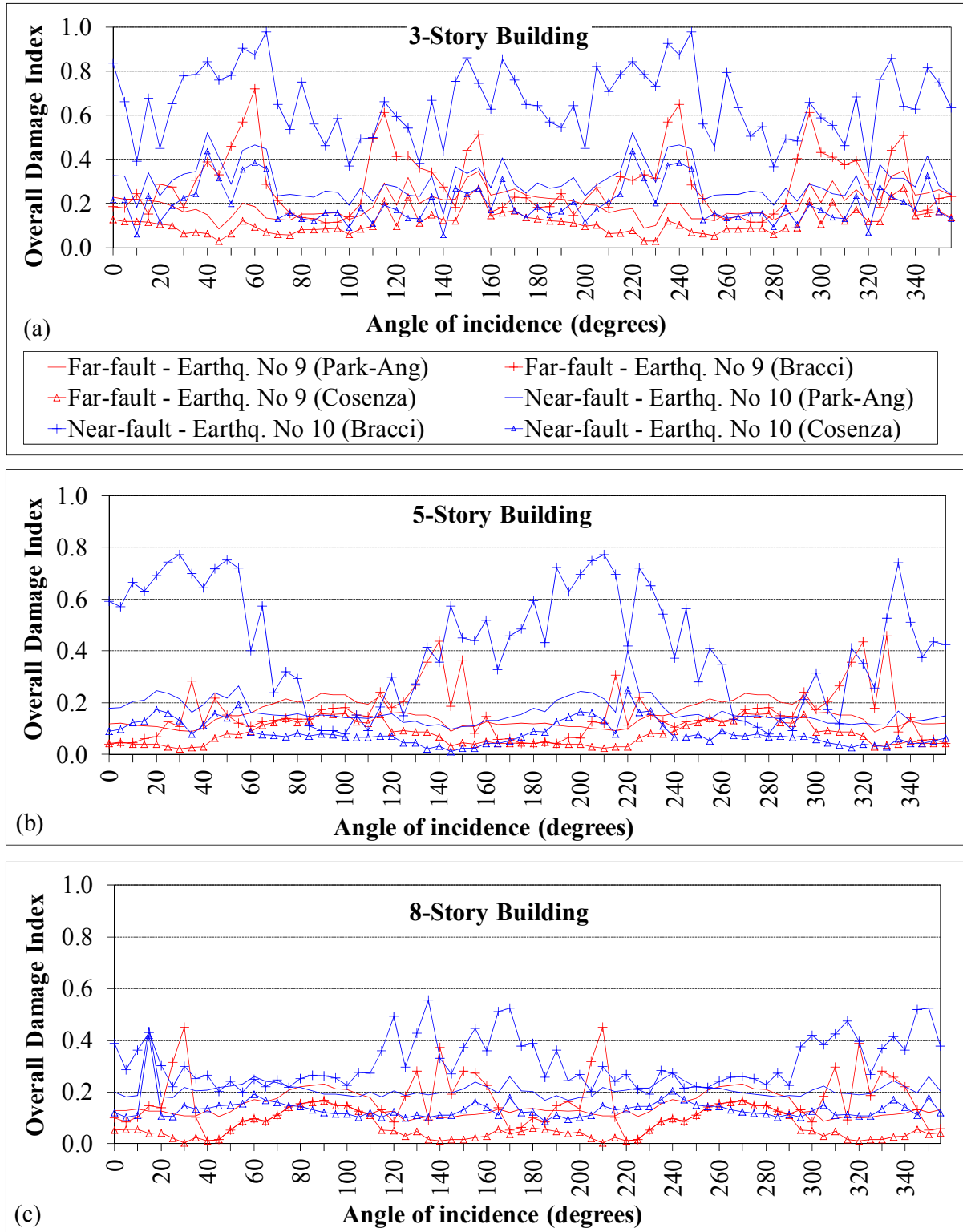


Figure 4: OSDI vs incident angle for earthquake records No9 (far-fault) and No10 (near-fault) for (a) the 3-story, (b) 5-story and (c) 8-story building

Concerning the 3-story building it is obvious from Figure 4a that the use of Bracci et al. damage index leads to the largest values of OSDI for the vast majority of incident angles, whereas the use of Cosenza et al. damage index leads to the smallest values. The same conclusion can be derived for the other two buildings under the near-fault earthquake record.

However, we observe that when the analyses are conducted using the far-fault ground motion there are certain angles of incidence for which Park and Ang gives larger values than the Bracci et al. damage index. See for example angles 0° - 15° , 55° - 110° and 235° - 290° (Figures 4b and 4c). It must be mentioned that the difference between the values produced by the three different definitions of the local damage index strongly depends on the seismic record and its orientation. For example, note that the three damage indices produce similar values of OSDI for the 5-story building (Figure 4b) when the near-fault record No10 is applied with angle of incidence 85° - 100° , whereas they lead to large differences when the orientation of the same earthquake record is 0° - 50° .

Furthermore, we can see that the damage state of the building is affected by the excitation angle for all the buildings under investigation. See for example that the OSDI of the 5-story building under the far-fault seismic record No10 using the Bracci et al. damage index is equal to 0.77 and 0.08 for incident angles 30° and 100° respectively (Figure 4b).

In order to generalize behavior trends, for each ground motion the value of the OSDI for incident angle $\theta=0^\circ$ ($OSDI_0$) as well as the maximum value of OSDI ($maxOSDI$) over all incident angles are determined. Then, the average values of the above quantities due to all the seismic records are calculated. The results are illustrated in Figures 5 and 6 for the three buildings under investigation. It must be mentioned that the aforementioned values are determined separately for the far and near fault records as well as for the three different definitions of the local damage index investigated in the present study.

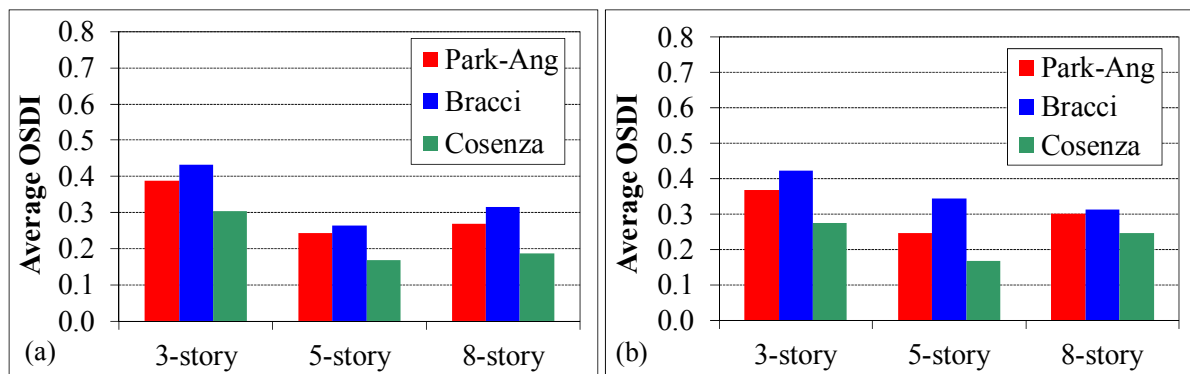


Figure 5: Average value of OSDI for incident angle $\theta=0^\circ$ determined using the three different LDI for (a) far-fault and (b) near-fault earthquake records

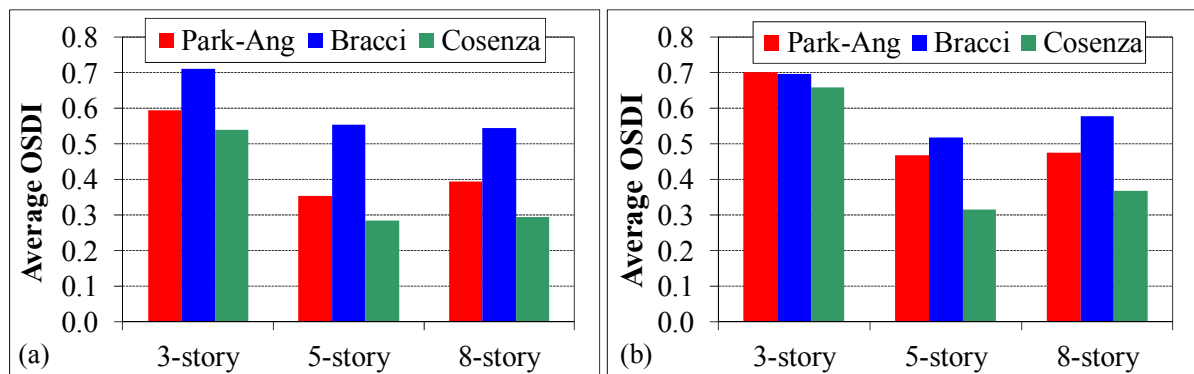


Figure 6: Average value of $maxOSDI$ over all incident angles determined using the three different LDI for (a) far-fault and (b) near-fault earthquake records

Figures 5 and 6 clearly indicate that the use of Bracci et al. damage index leads to the largest values of OSDI, whereas the use of Cosenza et al. damage index leads to the smallest values. The above conclusion is obvious for both $OSDI_0$ and $maxOSDI$. The difference between the three damage indices used in the present study depends on the number of stories and the type of the strong motion (far or near-fault), however no certain trend was observed. Note for example that the aforementioned difference is negligible for the $maxOSDI$ of the 3-story building under the near-fault records, whereas it becomes much larger for the $maxOSDI$ of the 5-story building under the far-fault records. This remark is very important, since different values of the OSDI imply different damage state of the structure. Furthermore, it is evident that the values of the three different OSDIs are larger for the 3-story building, something that can be attributed to the fact that, as can be seen in Figures 2a and 2b, the peaks of the most response spectra appear for values of period that is very close to the fundamental vibration period of the 3-story double symmetric structure. It is also interesting to notice that Figures 5 and 6 show no particular trend as far as the difference between the far and the near-fault records is concerned.

In order to better quantify the differences among the results produced for the 72 examined orientations of the ground motions, the maximum relative variation (MRV) of the OSDI for each seismic record is determined as:

$$MRV = (\max OSDI) / (\min OSDI) \quad (6)$$

where $\max OSDI$ and $\min OSDI$: maximum and minimum OSDI respectively over all seismic incident angles.

Then, the average and the maximum value of MRV for the 10 far-fault and the 10 near-fault records are computed. The results are presented in Figures 7 and 8.

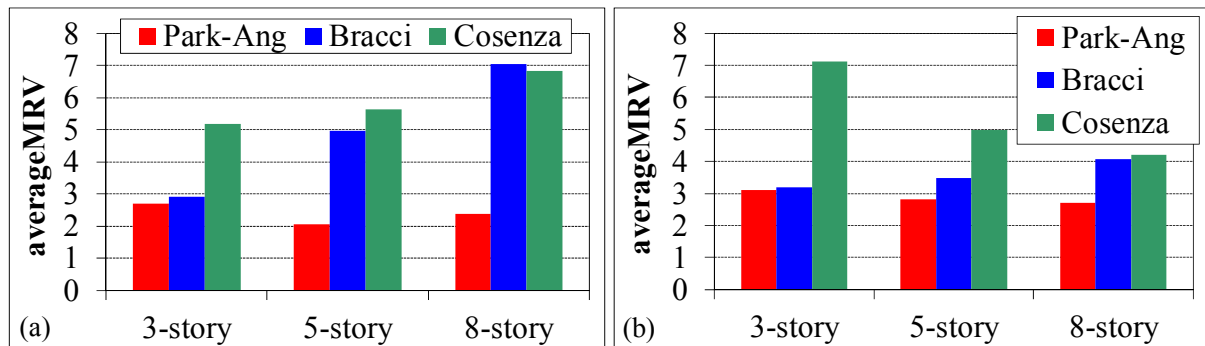


Figure 7: Average values of MRV for the OSDI determined using the three different LDI for (a) far-fault and (b) near-fault earthquake records

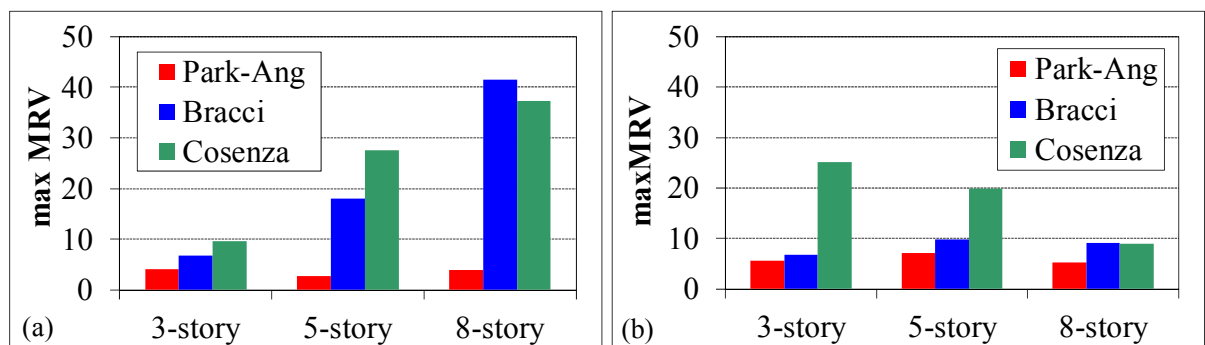


Figure 8: Maximum values of MRV for the OSDI determined using the three different LDI for (a) far-fault and (b) near-fault earthquake records

From Figures 7 and 8 it can be seen that the damage state of the building is strongly affected by the excitation angle for all the buildings under investigation. It is very interesting to notice that the average MRV can take the value of 7 (3-story building under near-fault records and 8-story building under far-fault records), whereas the maxMRV can take the value of 41 (8-story building under far-fault records).

The difference between the MRV determined using the three damage indices depends on the number of stories and the type of the strong motion (far or near-fault). The use of Cosenza et al. damage index leads to the largest values of MRV (with the exception of 8-story building), whereas the use of Park and Ang damage index leads to the smallest values. Moreover, concerning the far-fault records we can notice that the influence of the incident angle when the Bracci et al. and the Cosenza et al. damage indices are used becomes larger as the number of the stories increase. The opposite seems to happen for the Cosenza et al. damage index when the near-fault records are used. However, it is of great importance to notice that in most cases the most widely used Park and Ang damage index leads to the smallest influence of the number of stories

4 CONCLUSIONS

In the present research effort three damage indices for the R/C buildings are evaluated taking into account the incident angle of the strong motion. Three symmetric in plan R/C buildings are investigated: a low-rise (3 stories), a medium-rise (5 stories) and a high-rise (8 stories) one. The three buildings were analysed by nonlinear time-history analysis using 20 bi-directional earthquake ground motions, the horizontal accelerograms of each are applied along horizontal orthogonal axes forming 72 different angles with the structural axes. For each ground motion and incident angle, the local damage indices at every relevant cross section as well as the overall damage index of the building (OSDI) were computed using three different definitions of damage indices. The comparative assessment of the results leads to the following conclusions:

- The difference between the values of the three damage indices used in the present study varies depending on the number of stories, the earthquake ground motion and the incident angle.
- The use of Bracci et al. damage index leads to the largest values of OSDI, whereas the use of Cosenza et al. damage index leads to the smallest values for the vast majority of the incident angles and earthquake records.
- The damage state of the building strongly depends on the excitation angle. The influence of the incident angle depends on the damage index used, the number of stories and the strong motion.
- The most widely used Park and Ang damage index seems to be less influenced by the excitation angle as well as of the height of the building.

REFERENCES

- [1] K.G. Kostinakis, A.M. Athanatopoulou, Avramidis, Orientation effects of horizontal seismic components on longitudinal reinforcement in R/C Frame elements, *Natural Hazards and Earth System Sciences*, **12**, 1-10, 2012.
- [2] K.G. Kostinakis, A.M. Athanatopoulou, I.E. Avramidis, Evaluation of inelastic response of 3D single-story R/C frames under bi-directional excitation using different orientation schemes, *Bulletin of Earthquake Engineering*, DOI 10.1007/s10518-012-9392-5, 2012.

- [3] I.-K.M. Fontara, K.G. Kostinakis, A.M. Athanatopoulou, Some issues related to the inelastic response of buildings under bi-directional excitation, *Proceedings of the 15th World Conference on Earthquake Engineering*, Paper No: 3715, Lisbon, Portugal, September 24-28, 2012.
- [4] K. Morfidis, A.M. Athanatopoulou, I.E. Avramidis, Effects of seismic directivity within the framework of the lateral force procedure, *14th WCEE*, Beijing, China, October 12-17, 2008.
- [5] Y.J. Park, A.H.-S. Ang, Mechanistic Seismic Damage Model for Reinforced-Concrete. *Journal of Structural Engineering-ASCE*, **111**(4), 722-739, 1985.
- [6] S.K. Kunnath, A.M. Reinhorn et al, IDARC Version 3: A program for the inelastic damage analysis of RC structures, *Technical Report NCEER-92-0022*. National Centre for Earthquake Engineering Research, State University of New York, Buffalo NY, 1992.
- [7] J.M. Bracci, A.M. Reinhorn, J.B. Mander, S.K. Kunnath, Deterministic model for seismic damage evaluation of reinforced Concrete Structures, *Technical report NCEER-89-0033*, National Center for Earthquake Engineering Research, State University of New York at Buffalo, 1989.
- [8] E. Cosenza, G. Manfredi, R. Ramasco, The use of damage functionals in earthquake engineering: A comparison between different methods, *Earthquake Engineering and Structural Dynamics*, **22**, 855-868, 1993.
- [9] Eurocode 2: *Design of Concrete Structures, Part 1-1, General rules and rules for buildings*, European Committee for Standardization, Brussels, Belgium, 2004.
- [10] Eurocode 8: *Design of structures for earthquake resistance - Part 1, General rules, seismic actions and rules for buildings*, European Committee for Standardization, Brussels, Belgium, 2003.
- [11] RAF-Structural Analysis and Design Software v.3.3.2, TOL (Engineering Software House) Iraklion, Crete, Greece, 2012.
- [12] Pacific Earthquake Engineering Research Centre (PEER), Strong Motion Database. <http://peer.berkeley.edu/smcat/>, 2003.
- [13] The European Strong-Motion Database, http://www.isesd.hi.is/ESD_Local/frameset.htm, 2003.
- [14] J. Penzien, M. Watabe, Characteristics of 3-D earthquake ground motions, *Earthquake Eng. Struct. Dyn.*, **Vol. 3**, 365-373, 1975.
- [15] ASCE 41/06, Seismic rehabilitation of existing buildings, American Society of Civil Engineers 2009.
- [16] A. Otani, Inelastic Analysis of RC frame structures, *Journal of the Structural Division (ASCE)*, **100**(7), 1433–1449, 1974.
- [17] J.D. Pettings, M.J.N. Priestley, Dynamic Behaviour of Reinforced Concrete Frames Designed with Direct Displacement-Based Design, *Research Report No. ROSE-2005/02*, European School for Advanced Studies in Reduction of seismic Risk, 2005.
- [18] A.J. Carr, Ruaumoko – a program for inelastic time-history analysis, Program manual. Department of Civil Engineering, University of Canterbury, New Zealand, 2004.

- [19] Imbsen Software Systems, XTRACT: Version 3.0.5, Cross-sectional structural analysis of components, Sacramento, CA, 2006.
- [20] J.V. Amiri, Q.Y. Ahmadi et al, Assessment of reinforced concrete buildings with shear wall based on Iranian Seismic Code (Third edition), *J Appl Sci*, **8(23)**, 4274-4283, 2008.
- [21] K. Arjomandi, H. Estekanchi et al, Correlation Between Structural Performance Levels and Damage Indexes in Steel Frames Subjected to Earthquakes, *Scientia Iranica Transaction a-Civil Engineering*, **16(2)**, 147-155, 2009.
- [22] E. Yüksel E., M. Sürmeli, Failure analysis of one-story precast structures for near-fault and far-fault strong ground motions, *Bull Earthquake Eng.*, **8**, 937-953, 2010.
- [23] M.S. Williams, R.G. Sexsmith, Seismic Damage Indices for Concrete Structures: A State-of-the-Art Review, *Earthquake Spectra*, **11(2)**, 319-349, 1995.
- [24] S.L. Dimova, P. Negro, Seismic assessment of an industrial frame structure designed according to Eurocodes. Part 2: Capacity and vulnerability, *Eng Struct*, **27(5)**, 724-735, 2005.
- [25] A. Elenas, Correlation between seismic acceleration parameters and overall structural damage indices of buildings. *Soil Dyn Earthquake Eng*, **20(1-4)**, 93-100, 2000.